Aquatic Toxicology 101 (2011) 165–174

Contents lists available at ScienceDirect

Aquatic Toxicology

journal homepage: www.elsevier.com/locate/aquatox

AhR2-mediated, CYP1A-independent cardiovascular toxicity in zebrafish (*Danio rerio*) embryos exposed to retene

Jason A. Scott[a,1], John P. Incardona[b], Kathleen Pelkki[c], Sally Shepardson[c], Peter V. Hodson[a,d,*]

[a] Department of Biology, Queen's University, 116 Barrie Street, Kingston, ON K7L 3N6, Canada
[b] Ecotoxicology and Environmental Fish Health Program, Environmental Conservation Division, Northwest Fisheries Science Center, National Oceanic and Atmospheric Administration, 2725 Montlake Boulevard, Seattle, WA 98112, United States
[c] Department of Biology, Saginaw Valley State University, 7400 Bay Road, University Center, MI 48710, United States
[d] School of Environmental Studies, Queen's University, 116 Barrie Street, Kingston, ON K7L 3N6, Canada

ARTICLE INFO

Article history:
Received 26 April 2010
Received in revised form
17 September 2010
Accepted 25 September 2010

Key words:
Alkylated polycyclic aromatic hydrocarbons
Retene
Aryl hydrocarbon receptor
Cytochrome P450 1A
Embryotoxicity
Cardiac development

ABSTRACT

In the embryo-larval stages of fish, alkylphenanthrenes such as retene (7-isopropyl-1-methylphenanthrene) produce a suite of developmental abnormalities typical of exposure to 2,3,7,8-tetrachlorodibenzo-*p*-dioxin (TCDD), including pericardial and yolk sac edema, cardiovascular dysfunction, and skeletal deformities. To investigate the mechanism and target tissue of retene toxicity, we used observational, histological, and protein knockdown techniques in zebrafish (*Danio rerio*) embryos. The primary overt signs of toxicity are pericardial edema and reduced blood flow, first observed at 36 h post-fertilization (hpf). The most pronounced effects at this stage are a reduced layer of cardiac jelly in the atrium and reduced diastolic filling. Conversely, an increased layer of cardiac jelly is observed at 72 hpf in retene-exposed embryos. Induction of cytochrome P4501A (CYP1A) is apparent in a subset of cardiomyocytes by 48 hpf suggesting that early cardiac effects may be due to AhR activation in the myocardium. Myocardial CYP1A induction is transient, with only endocardial induction observed at 72 hpf. Knockdown of *cyp1a* by morpholino oligonucleotides does not affect retene toxicity; however, *ahr2* knockdown prevents toxicity. Thus, the mechanism of retene cardiotoxicity is AhR2-mediated and CYP1A-independent, similar to TCDD; however, the onset and proximate signs of retene toxicity differ from those of TCDD. Retene cardiotoxicity also differs mechanistically from the cardiac effects of non-alkylated phenanthrane, illustrating that alkyl groups can alter toxic action. These findings have implications for understanding the toxicity of complex mixtures containing alkylated and non-alkylated polycyclic aromatic hydrocarbons.

© 2010 Elsevier B.V. All rights reserved.

1. Introduction

Alkylphenanthrenes are polycyclic aromatic hydrocarbon (PAH) constituents of crude oil and have been implicated in the toxicity of crude oil to the early life stages of fish (Carls et al., 1999; Heintz et al., 1999; Hodson et al., 2007a). Retene (7-isopropyl-1-methylphenanthrene) is a C-4 phenanthrene derived from both natural and anthropogenic sources and a useful model for studying alkylphenanthrene toxicity. It can occur naturally in crude oil, and in sediments at high concentrations near pulp and paper mills (Leppanen and Oikari, 1999). Exposures to crude oil or to retene produce a syndrome characterized by cardiovascular dysfunction, pericardial and yolk sac edema, and craniofacial and spinal deformities (Billiard et al., 1999; Carls et al., 1999; Heintz et al., 1999; Incardona et al., 2005; Incardona et al., 2009). These signs overlap considerably with the effects of exposure to persistent organochlorine contaminants, including 2,3,7,8-tetrachlorodibenzo-*p*-dioxin (TCDD or dioxin). Dioxin-like toxicity in zebrafish embryos is mediated via the aryl hydrocarbon receptor 2 (AhR2, the functional AhR isoform; Prasch et al., 2003; Dong et al., 2004; Antkiewicz et al., 2006), a ligand-activated transcription factor that initiates the expression of a battery of genes involved in xenobiotic metabolism (e.g., cytochrome P450 1A) and in normal development and homeostasis (Fernandez-Salguero et al., 1997; Hahn, 1998; Walisser et al., 2004). Upon activation, the AhR translocates into the nucleus and heterodimerizes with the AhR nuclear translocator. The resulting complex binds to xenobiotic responsive elements (XREs) in the promotor region of AhR-responsive genes, initiating transcription (Hahn, 1998). For dioxin-like compounds, the mechanism down-

* Corresponding author at: Department of Biology, Queen's University, 116 Barrie Street, Kingston, ON K7L 3N6, Canada. Tel.: +1 613 533 6129; fax: +1 613 533 6090.
E-mail addresses: 4jas4@queensu.ca (J.A. Scott), John.Incardona@noaa.gov (J.P. Incardona), pelkki@svsu.edu (K. Pelkki), sps@svsu.edu (S. Shepardson), peter.hodson@queensu.ca (P.V. Hodson).
[1] Present address: College of Pharmacy, University of New Mexico Health Sciences Center, MSC09 5360, 1 University of New Mexico, Albuquerque, NM 87131, United States.

0166-445X/$ – see front matter © 2010 Elsevier B.V. All rights reserved.
doi:10.1016/j.aquatox.2010.09.016

stream of AhR activation remains largely uncertain; however, it is independent of CYP1A activity (Carney et al., 2004). In contrast, the developmental toxicity of non-alkylated (parent) tricyclic PAHs such as phenanthrene, as well as crude oil-derived mixtures enriched with parent PAHs, were found to be independent of the AhR pathway (Incardona et al., 2005).

As oil weathers over time, the resulting aqueous mixtures shift from being dominated by more water-soluble parent compounds to become enriched with alkylated PAHs (Carls and Meador, 2009; Short and Heintz, 1997). While phenanthrene (non-alkylated retene) is a poor AhR ligand (and produces AhR-independent toxicity), retene (and probably other alkylphenanthrenes) competes with TCDD for binding to the AhR of some species (Billiard et al., 2002). Thus, a key question is whether the toxic mechanisms associated with petrogenic PAH mixtures differ according to the relative abundance of parent and alkylated compounds. Another complicating factor for understanding PAH toxicity is that organochlorines are poor substrates for CYP1A, whereas alkylphenanthrenes are rapidly metabolized by CYP1A (Fragoso et al., 1999; Hawkins et al., 2002). Xenobiotic metabolism by CYP1A enzymes could contribute to toxicity through the production of reactive oxygen species (ROS) and/or reactive metabolite intermediates (Di Giulio et al., 1995).

The involvement of AhR and CYP1A in alkylphenanthrene toxicity is suggested by structure–activity relationship studies of alkyl-PAHs, which identify a possible link between the toxicity of alkylphenanthrenes and their binding affinity to the AhR. AhR-binding alkylphenanthrenes produced dioxin-like toxicity in Japanese medaka (*Oryzias latipes*), which generally follows a rank order of potency in accordance with an increase of lipophilicity (Turcotte et al., 2010; Kiparissis et al., 2001). Furthermore, the byproducts of metabolism implicate CYP1A in the mechanism of retene toxicity (Hawkins et al., 2002; Brinkworth et al., 2003; Bauder et al., 2005; Hodson et al., 2007b). In retene-exposed rainbow trout (*Oncorhynchus mykiss*) embryos, CYP1A induction precedes signs of toxicity (Brinkworth et al., 2003), and toxicity decreases after chemical inhibition of CYP1A enzyme activity (Hawkins et al., 2002; Hodson et al., 2007b). In addition, Bauder et al. (2005) implicate ROS-induced oxidative stress in retene toxicity, as there are decreases in glutathione and Vitamin E concentrations in retene-exposed trout larvae, and retene toxicity is reduced when larvae were co-treated with Vitamin E.

Although retene toxicity to the early life stages of zebrafish was described previously (Billiard et al., 1999), it was primarily late-stage larval effects, with little insight into the proximate signs of dioxin-like toxicity during the embryonic stages of development. Thus, the aims of this study were to comprehensively study the mechanisms of retene toxicity by: (1) identifying both proximal signs and progression of cardiovascular toxicity using observational, histological, and immunofluorescent analyses; and (2) directly investigating the involvement of CYP1A and AhR using antisense morpholino oligonucleotides. Using retene as a model alkyl-PAH, the ultimate aim of this study was to provide insight into the changing toxicity of crude oil during weathering, in which volatile compounds are lost and concentrations of alkyl-PAHs are enriched.

2. Materials and methods

2.1. Chemicals

Retene (98% pure) was obtained from ICN Biomedical (Aurora, ON). Dimethylsulfoxide (DMSO; Sigma, St. Louis, MO) was used as a carrier solvent for retene. Stock solutions were prepared at a concentration of 20 mg retene/mL DMSO, and were stored at 4 °C.

2.2. Morpholino knockdown

Antisense morpholino oligonucleotides (Gene Tools, Philomath, OR) were used to sterically block the translation of AhR2 and CYP1A mRNAs, thus knocking down the gene product. The morpholino oligonucleotide sequences (Teraoka et al., 2003) were as follows: AhR2 (*ahr2-MO*), 5′-TGTACCGATACCCGCCGACATGGTT-3′; CYP1A (*cyp1a-MO*), 5′-TGGATACTTTCCAGTTCTCAGCTCT-3′; and generic standard control (*std-MO*), 5′-CCTCTTACCTCAGTTACAATTTATA-3′. The eggs were injected as described by Incardona et al. (2006) and were maintained at 28.5 °C until observational analysis.

2.3. Zebrafish exposures

Maintenance of wild-type AB, *nacre*, and Tg(*fli1-EGFP*) strains of zebrafish and egg collection protocols are described elsewhere (Linbo, 2009). The *nacre* mutation and Tg(*fli1-EGFP*) transgene are carried in an AB strain background. After collection and/or injection, the eggs were incubated at 28.5 °C until 50% epiboly, at which time they were exposed to 12.5 μg/mL retene or DMSO (0.0006%, v/v), a high concentration chosen to ensure that the fish would respond to retene and that the sequence of responses could be followed. At the concentration used, most of the retene would be absorbed to surfaces and would partition into water to the limits of its solubility, about 15–16 μg/L based on partitioning experiments (Kiparissis et al., 2003). The focus of this mechanistic study was to ensure that toxicity occurred within the constraints of very small exposure systems suited to zebrafish embryos, and not on producing data to establish water quality criteria, as has already been done (Brinkworth et al., 2003; Kiparissis et al., 2003).

The exposures were carried out in glass Petri dishes with up to 50 embryos/dish, equivalent to about 1 g biomass/L in 40 mL of test solution, which was renewed daily. Retene exposures were run in triplicate, and all injected DMSO controls were run in duplicate. For quantification of cardiac effects, three replicate groups of 20 embryos each were exposed to either DMSO or 12.5 μg/mL retene. No early embryonic mortality was observed in DMSO-exposed controls, but 15% of retene-exposed embryos died before 24 hpf. Due to time and egg number constraints, there was only one replicate of uninjected DMSO controls containing 45 eggs. This would not affect the interpretation of our results, as all morpholino-injected DMSO controls showed no signs of toxicity. No toxicity has been observed in previous DMSO exposures at similar concentrations (data not shown). Retene exposures for observation of cardiac effects were repeated in three independent experiments, all with qualitatively similar results documented by representative digital videos. The overall frequency of edema and the degree of cardiac dysfunction were consistent across experiments. Changes in atrial wall thickness were observed qualitatively in each retene exposure assay. Cardiac contractility and atrial wall thickness were quantified in one experiment (see below).

2.4. Stereo- and confocal microscopy

Embryos were mounted in 3% methylcellulose, and digital video and still images collected at 24, 36, 48 and 72 hpf, as previously described (Incardona et al., 2006). Pericardial edema was measured at 72 hpf by outlining the boundaries of the pericardial sac and quantifying the number of pixels using Image J software (U.S. National Institute of Health, Bethesda, MD). Heart rate was quantified in unanesthetized embryos by counting beats over a 15-s interval. Contractility was assessed by measuring fractional shortening, an indicator of systolic contractility normalized to chamber diameter (Bendig et al., 2006). End-diastolic and end-systolic diameters of the atrium were measured in digital videos using ImageJ, and fractional shortening calculated as

(end-diastolic diameter) − (end-systolic diameter)/(end-diastolic diameter) × 100. For measurements of atrial wall thickness, frames in digital videos were chosen at end-diastole, and the wall thickness measured in ImageJ at a consistent point on the anterior side at the dorsal-ventral midpoint. Immunofluorescence (at 72 hpf) and endothelial fluorescence of Tg(*fli1-EGFP*) embryos (at 52 hpf) were imaged using a Zeiss LSM 5 confocal microscope. The embryos were fixed in 4% paraformaldehyde and processed for immunofluorescence as previously described (Incardona et al., 2006). The primary antibodies used for immunofluorescence were anti-fish CYP1A monoclonal C10-7 (Caymen Chemical, Ann Arbor, MI), anti-myosin heavy chain monoclonal MF20, and anti-atrial myosin heavy chain S46 (both from Developmental Studies Hybridoma Bank, University of Iowa). The secondary antibodies were AlexaFluor488-conjugated goat-anti-mouse IgG_3 (for C10-7), AlexaFluor488-conjugated goat-anti-mouse IgG_1 (S46) and AlexaFluor568-conjugated goat-anti-mouse IgG_{2b} (MF20; all from Invitrogen-Molecular Probes, Eugene, OR).

2.5. Histology

At 72 hpf, zebrafish embryos were fixed in 4% paraformaldehyde, washed in PBT (phosphate buffered saline, 0.2–0.5% Triton X-100) and dehydrated in a graded series of ethanol concentrations at 10 min intervals at room temperature. The embryos were placed in propylene oxide (2 × 10 min), followed by an embedment in Epon-Araldite. The specimens were sliced at 500 nm using a RMC MT6000 ultramicrotome. The sections were thermally adhered to a glass slide and stained with 1% filtered toluidine blue. The sections were viewed with an Olympus BX51 microscope and photographs were digitally captured using an Olympus QColor 5 camera and QCapture Pro software (Ver. 5.1.1.14, Media Cybernetics, Inc., Bethesda, MD). The cross-sectional size of atrial walls, and ventricles were measured in pixels by outlining the boundaries of the tissues using Image J software (U.S. National Institute of Health, Bethesda, MD). The atrial wall thickness was calculated by subtracting the lumen area from the area measured at the outer boundary of the atrium (i.e., myocardial layer).

2.6. Statistics

The prevalence and severity of pericardial edema were analyzed using a two-way analysis of variance, followed by a Student–Newman–Keuls multiple pairwise comparison. Heart chamber measurements were analyzed by Student's *t* test or one-way ANOVA followed by a Tukey–Kramer Honestly Significant Differences test (alpha = 0.05). Statistical analyses were performed using SigmaStat Ver. 1.0 (Jandel Scientific, Chicago, IL; $p < 0.05$) or JMP 6.0.2 for Macintosh (SAS Institute, Inc., Cary, NC).

3. Results

3.1. Retene toxicity

Retene embryotoxicity was first observed at 36 hpf, with pericardial edema and reduction in blood flow as the proximate signs of toxicity (Supplemental Movie S1). At this stage, two degrees of cardiac impairment were observed: 35 ± 4% of retene-exposed embryos had markedly reduced circulation with stasis of erythrocytes in the common cardinal vein (Fig. 1a,b), while the remainder showed slower entry of erythrocytes into the atrium relative to controls (Movie S2). The stasis of erythrocytes in the common cardinal vein of retene-exposed embryos was due to reduced atrial filling (Movie S1, Fig. 1d), but there was no difference in atrial contractility between retene exposed embryos and controls, both of which had atrial fractional shortening values of 23 ± 3% (retene $n = 8$, control $n = 7$). However, the atria in these embryos appeared slightly dilated with a reduction in the thickness of the cardiac jelly (extracellular matrix) between the myocardium and endocardium in the anterior portion of the chamber (Fig. 1c,d). Measurement of the anterior atrial wall thickness in digital images (e.g. Fig. 1c,d) showed a relationship among retene treatment, wall thickness, and atrial function (Table 1). Control (DMSO-exposed) embryos had an average wall thickness of 13.1 ± 0.6 μm, while the atrial wall was reduced to 8.1 ± 0.5 μm in retene-exposed embryos with poor atrial filling, and 10.8 ± 0.9 μm in retene-exposed embryos that had better atrial filling without marked dilation. In some retene-exposed embryos, the ventricles appeared smaller at 36 hpf (data not shown). By 48 hpf, 90 ± 2% of retene-exposed embryos showed reduced circulation (i.e., stasis in the cardinal vein), with reduced ventricular size more apparent and the atria remaining dilated (Fig. 1e,f). All retene-exposed embryos with reduced circulation at this stage (46/51) showed thinner atrial walls (e.g. Fig. 1f). There was no difference in heart rate at 48 hpf, with a rate of 162 ± 3 beats/min for DMSO-exposed controls and 165 ± 2 beats/min for retene-exposed embryos ($p = 0.17$, $n = 15$ each). At 72 hpf the morphology of the heart in retene-exposed embryos was distinctly different, with a markedly reduced ventricle and underdevelopment of the bulbus arteriosus (Fig. 1g,h). By this time, the atria appeared to have an increased thickness of cardiac jelly, apparent in both live specimens and in histological sections (Fig. 2), and the ventricular myocardium was thinner than in controls. Quantification in five embryos showed a significant increase in the extracellular space between the atrial myocardium and endothelium ($p = 0.003$; Fig. 2a,b). There was evidence for a disruption in erythropoiesis in retene-exposed embryos; only round primitive erythrocytes were apparent, in contrast to the more flattened, ovoid definitive erythrocytes observed in control embryos (Fig. 2c,d).

Table 1
Retene-induced impairment of atrial function at 36 hpf correlates with atrial wall thickness.

Treatment	Atrial function	Wall thickness (μm)[a]	*N*
DMSO	Normal	13.1 ± 0.6[A]	6
12.5 μg/mL retene	Intermediate	10.8 ± 0.9[B]	7
12.5 μg/mL retene	Poor	8.1 ± 0.5[C]	6

[a] Values are mean ± SE; ANOVA showed an effect of treatment ($p = 0.0002$) and letters indicate statistically different groups in post hoc means comparison by Tukey–Kramer HSD test (alpha = 0.05).

By 72 hpf there was a significant difference in the prevalence and severity of pericardial edema in retene-exposed embryos ($p < 0.001$; Fig. 3), except in *ahr2* morphants (discussed below). Retene-induced craniofacial deformities (reduced lower jaw) and intracranial hemorrhaging were also observed.

3.2. Role of AhR2 and CYP1A

At 48 hpf there was widespread CYP1A immunoreactivity in the epidermis (Fig. 4a) and vascular endothelium (data not shown) of uninjected embryos exposed to retene. Consistent with previous studies, injection of *cyp1a* morpholino resulted in an overall marked reduction in CYP1A immunoreactivity throughout the epidermis and vasculature, including the endocardium (Fig. 4b and data not shown). In *ahr2* morphants, the epidermal expression of CYP1A was reduced; however, CYP1A expression was still observed in the vasculature and eye (Fig. 4c). In the heart, strong CYP1A immunofluorescence was observed in the endocardium of both chambers (Fig. 5c), while CYP1A induction was evident in a subset of ventricular myocardial cells (Fig. 5c). In five embryos examined in detail, optical sectioning showed that CYP1A immunofluorescence was detectable consistently in a patch of myocardial cells that extended along the anterior outer curvature of the ventri-

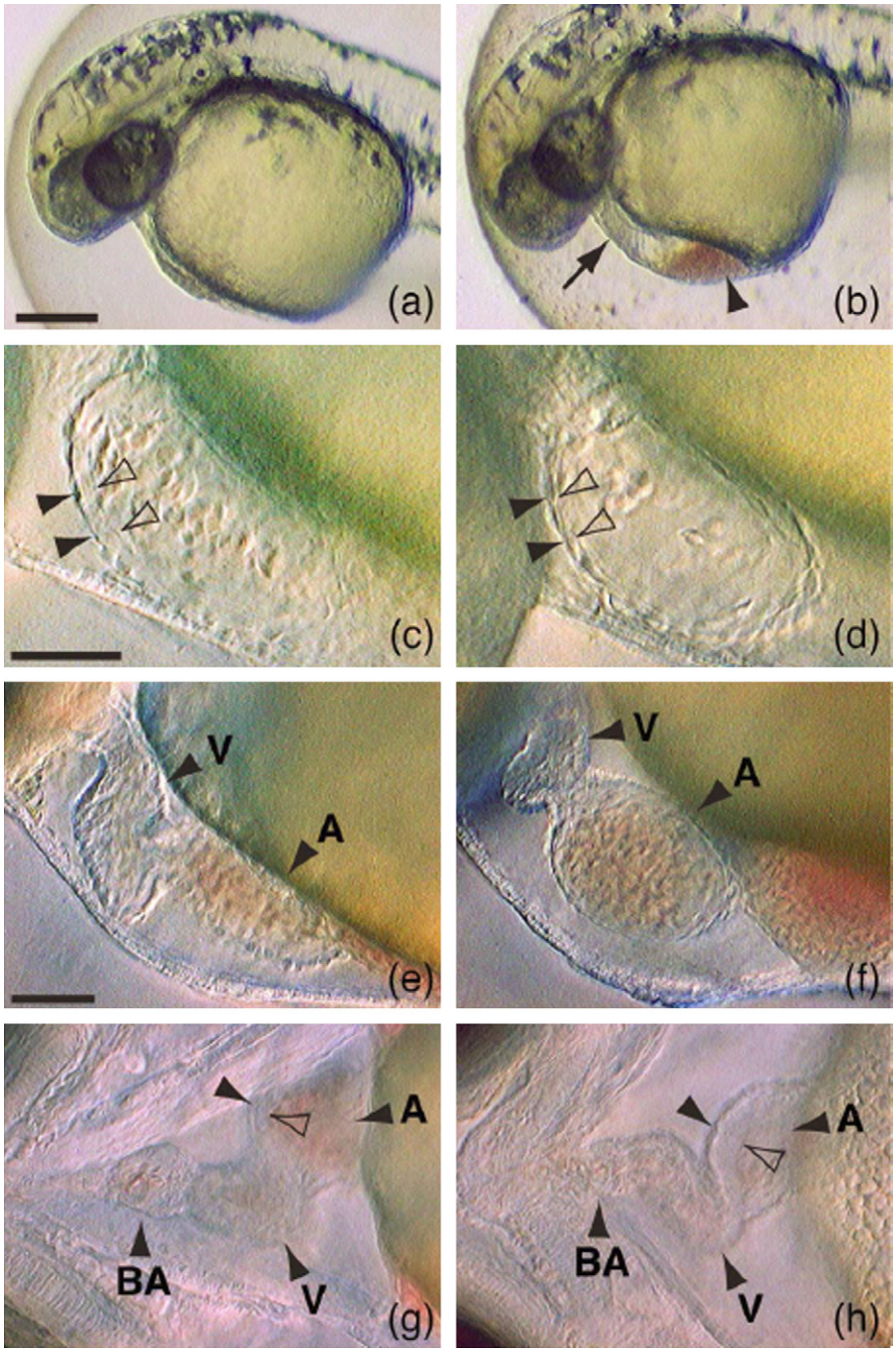

Fig. 1. Cardiac defects resulting from retene exposure. Embryos exposed to DMSO (a, c, e, g) and to retene (b, d, f, h) at 36 hpf (a-d), 48 hpf (e, f) and 72 hpf (g, h). Left lateral views are shown in a–f, with ventral views shown in g and h and anterior to left in all images. In c–h, images are single frames taken from digital video at the end of atrial diastole, i.e., at peak relaxation of the atrium. (a, b) Arrow indicates pericardial edema in retene-exposed embryo. (c, d) Atrium at 36 hpf is slightly dilated in retene-exposed embryo with a reduced number of erythrocytes in the lumen, and shows reduced cardiac jelly between the myocardium (filled arrowheads) and the endocardium (unfilled arrowheads). (e, f) Dilated atrium (*A*) and small ventricle (*V*) in retene-exposed embryo at 48 hpf. (g, h) Poorly developed bulbus arteriosus (*BA*) and thicker cardiac jelly (space between filled and unfilled arrowheads) in the atrium (*A*) of retene-exposed embryos. See also Supplemental Movie S1. Scale bars are 0.2 mm (a, b) and 50 μm (c, d; e–h). Images are representative of >50 embryos for each treatment.

cle (OC, Fig. 5a,b). CYP1A induction was not detected in the atrial myocardium. However, we cannot unequivocally rule out atrial AhR activation, because the high intensity of the endocardial CYP1A immunofluorescence may have obscured any weaker signals in the myocardium. At 72 hpf, retene-exposed embryos showed only endocardial CYP1A immunofluorescence (Fig. 5d), with an absence of induction throughout the ventricular myocardium. This combined loss of epidermal CYP1A induction with retention of vascular endothelial induction in ahr2 morphants is similar to that observed with the 4-ring PAHs chrysene and benz(a)anthracene (Incardona et al., 2005; Incardona et al., 2006).

Knockdown of AhR2 by *ahr2*-MO knockdown prevented retene toxicity in zebrafish embryos (Fig. 6h). The prevalence and severity of pericardial edema in *ahr2* morphants were significantly lower than those of uninjected embryos exposed to retene ($p < 0.001$), and were not different from those of control embryos (Figs. 3 and 6). Conversely, *cyp1a*-MO knockdown did not alleviate toxicity in retene-exposed embryos (Figs. 3 and 6h), as there was no significant

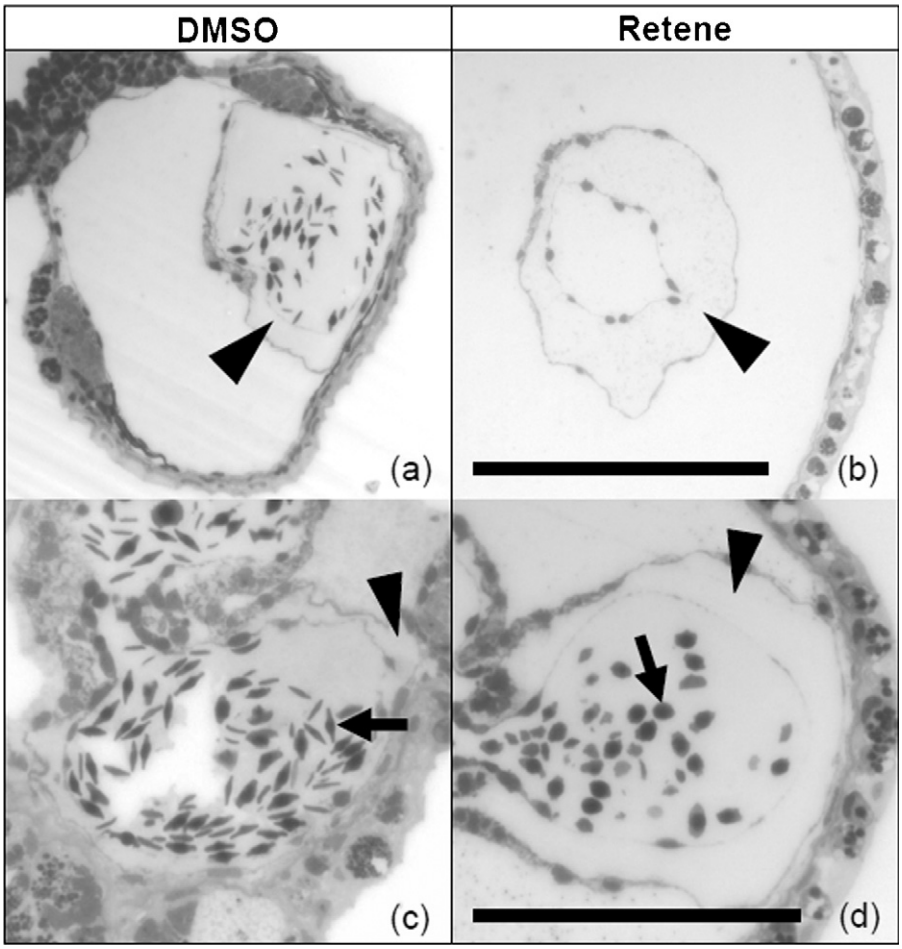

Fig. 2. (a,b) Atrium wall thickness and (c,d) erythrocyte morphology of retene- and DMSO (0.0006%, v/v)-exposed zebrafish embryos at 72 hpf. Arrowhead, atrial wall; arrow, erythrocyte. Scale bar = 0.1 mm. Images are representative of 5 embryos per treatment.

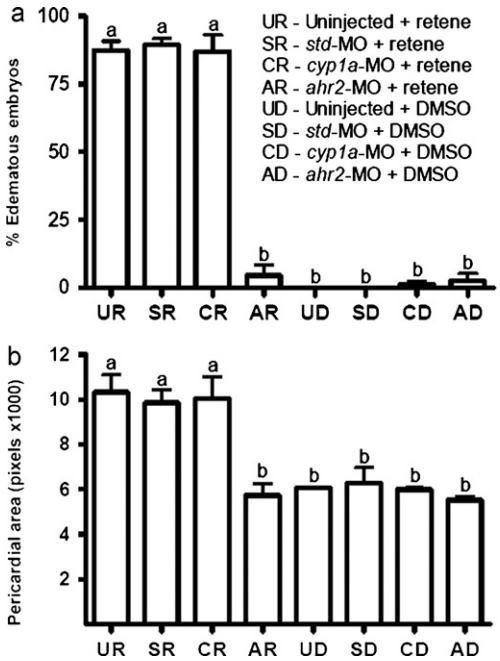

Fig. 3. Zebrafish embryotoxicity as described by (a) prevalence and (b) severity of pericardial edema at 72 hpf. The data represent the (a) mean percent of embryos displaying edema and (b) mean pericardial area ± SE (N = 1–3 replicates, 19–50 embryos per replicate; $p < 0.05$).

difference in toxicity between *cyp1a* morphants and uninjected embryos exposed to retene. As expected, the generic standard control morpholinos did not influence toxicity and there was no significant toxicity observed in all DMSO controls (Figs. 3 and 6a–d). Thus, the toxicity of retene to the early developmental stages of zebrafish is mediated by an AhR2-dependent and CYP1A-independent mechanism.

4. Discussion

4.1. Retene embryotoxicity

Retene causes cardiogenic edema in the embryo-larval stages of zebrafish, in agreement with previous studies of zebrafish using similar static daily renewal protocols (Billiard et al., 1999), and with studies of medaka by partition-controlled delivery (Kiparissis et al., 2003), and trout by continuous-flow desorption columns (Brinkworth et al., 2003). All species display similar signs of toxicity as those described herein, although the present study includes a greater level of detail.

The onset of toxicity occurs sometime between 30 and 36 hpf, with the proximate signs of toxicity first appearing at 36 hpf. The earliest effect appears to be a loss of pump function of the heart, without a change in heart rate or myocardial contractility. The most pronounced effect appears to be in the atrium, which shows a reduced layer of cardiac jelly, an extracellular matrix secreted by the myocardium that is important for the elasticity of the early tubular heart (Barry, 1948). In contrast, by 72 hpf the atrium has an

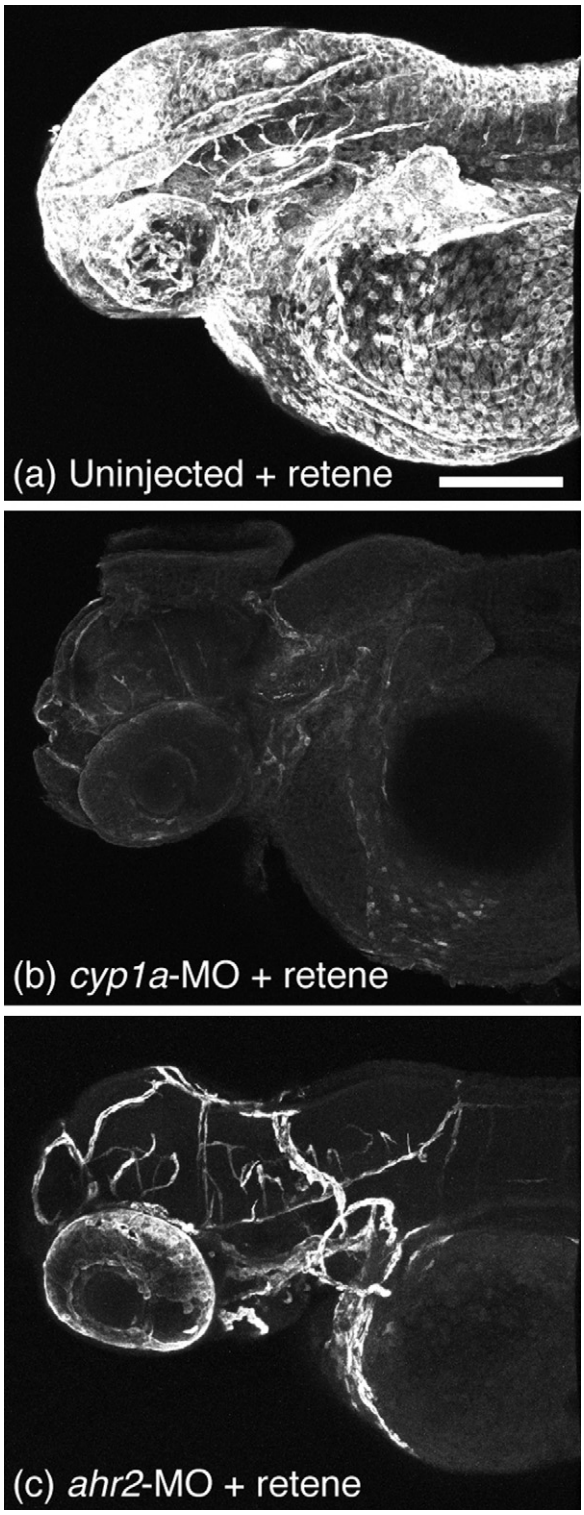

Fig. 4. CYP1A immunofluorescence in uninjected, *cyp1a*-MO- and *ahr2*-MO-injected zebrafish embryos exposed to retene. Images are representative of at least 20 embryos per treatment. Only weak background fluorescence was observed in DMSO-exposed controls (not shown). Similar epidermal and vascular endothelial patterns were observed in the trunk for each treatment group (not shown). Scale bar = 0.1 mm.

increased layer of cardiac jelly in retene-exposed embryos, which was most readily apparent in histological sections. Recent studies in zebrafish and chick embryos suggest that the early tubular heart functions as a suction pump dependent on elasticity (Forouhar et al., 2006; Männer et al., 2008), consistent with properties conferred by the cardiac jelly. Although the role of cardiac jelly has not yet been assessed specifically in zebrafish, a parsimonious explanation for the reduced atrial diastolic filling and dilation observed in retene-exposed embryos at 36 hpf is due to a loss of elasticity of the atrium secondary to a reduced deposition of cardiac jelly. This is also consistent with the observed functional relationship between atrial filling and wall thickness. While effects on the ventricle appeared minimal at 36 hpf, altered ventricular morphology and function were dramatic by 48–72 hpf. It is thus unclear if the later morphology of the atrium is due to intrinsic effects of retene exposure, or secondary to ventricular dysfunction. The apparent paradoxical increase in atrial cardiac jelly observed at 72 hpf could be compensatory.

Two of the proximate signs of retene toxicity are similar to those observed in 3,3′,4,4′,5-pentachlorobiphenyl (PCB126) and TCDD exposures. In PCB126 embryos, pericardial edema appears by 36 hpf (Grimes et al., 2008), similar to retene. However, in TCDD-exposed zebrafish embryos, the first measurable changes occur are at 48 hpf and include a decrease in cardiomyocyte number (Antkiewicz et al., 2005) and regurgitation of erythrocytes through the atrioventricular valve (Mehta et al., 2008). TCDD-induced pericardial edema typically does not present until 72 hpf (Belair et al., 2001; Prasch et al., 2003; Antkiewicz et al., 2005). The sequence of events induced through activation of the AhR by PCB126 and TCDD appears to be a failure of ventricular cardiomyocyte proliferation that normally occurs between 48 and 72 hpf (Hu et al., 2000), followed by an incomplete looping and formation of the bulbus arteriosus, ultimately leading to complete heart failure and development of the characteristic string-like cardiac morphology (Antkiewicz et al., 2005; Jönsson et al., 2007; Grimes et al., 2008; Mehta et al., 2008). The AhR-dependent cardiac effects of retene exposure are generally less severe, but are visible at an earlier developmental stage. Continuous exposure to retene beginning shortly after fertilization results in a transient induction of CYP1A in a subset of cardiomyocytes, evident by 48 hpf but absent at 72 hpf. It is thus most likely that the functional defects resulting from retene exposure are due to AhR activation in either the ventricular or atrial myocardium. A simple interpretation is that activation of AhR2 in the myocardium up to 48 hpf results in disruption of gene expression required for normal cardiac jelly deposition. The decay of myocardial CYP1A in the presence of robust epidermal and endothelial CYP1A expression, coupled with the increase in atrial cardiac jelly at 72 hpf suggests that by this point, the myocardium may be protected from on-going retene exposure. Although the pattern of CYP1A induction by PCB 126 and TCDD in the heart has not been characterized in detail, these effects of retene are consistent with those observed for another AhR binding PAH, benz[*a*]anthracene (Incardona et al., 2006).

The differences between retene and TCDD may reflect differences in toxicokinetics in addition to AhR binding affinity. First, studies with TCDD describe the effects of a transient exposure shortly after fertilization, followed by transfer to clean water (Antkiewicz et al., 2005; Belair et al., 2001; Henry et al., 1997.). Because TCDD is not metabolized, this results in an initial load that is presumably concentrated in the yolk, then distributed to the growing embryo. In this study, embryos were exposed to retene continuously with static renewal, and retene is metabolized by CYP1A. Although TCDD is slightly more hydrophobic (retene K_{ow} = 6.4, TCDD K_{ow} = 6.8), it is likely that these different exposure protocols would result in different tissue distributions of active ligand. Moreover, it is likely that CYP1A induction after retene exposure would alter the pattern of active ligand. After 48 h retene may not reach the myocardium because of retene metabolism in endocardial cells, which would affect the timing and degree of cardiac dysfunction in relation to the pattern of cardiac CYP1A induction. However, it is important to note that a CYP1A-independent effect in

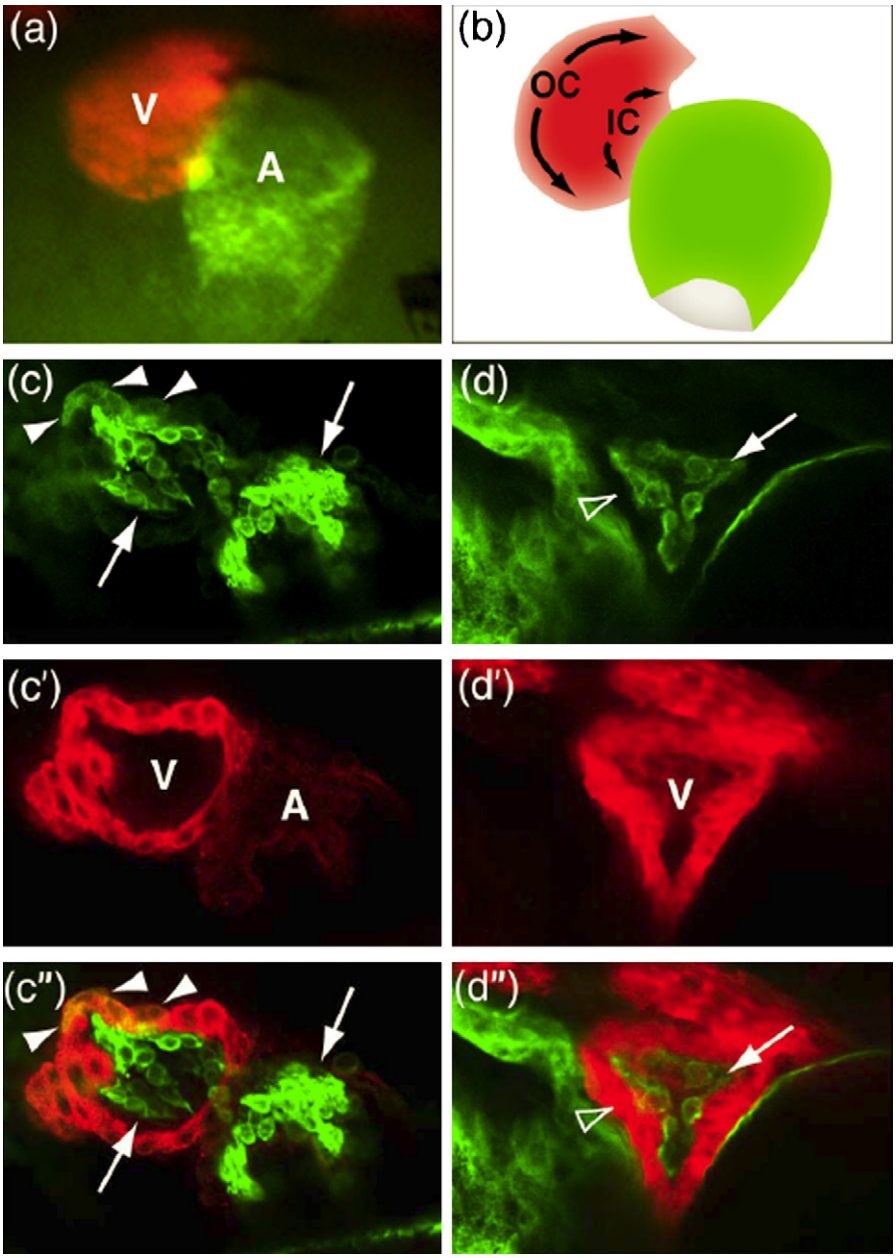

Fig. 5. CYP1A immunofluorescence in the heart of retene-exposed embryos. (a) The morphology of the heart at 48 hpf shown with chamber-specific antibodies MF20 (red) and S46 (green). (b) Both the atrium (*A*) and the ventricle (*V*) have a convex outer curvature (*OC*) and a concave inner curvature (indicated for the ventricle). (c, d) CYP1A immunofluorescence (green), (c′, d′) myosin heavy chain immunofluorescence (red) marks cardiomyocytes, (c″, d″) merged images. (c) At 48 hpf CYP1A immunofluorescence was present in endocardial cells of both chambers (arrows), and in myocardial cells in the anterior part of the ventricular OC (arrowheads). (d) At 72 hpf CYP1A was detected in endocardial cells (arrow), but not the myocardium (unfilled arrowhead). Images are representative of at least 20 embryos; OC staining was assessed in 5 embryos. (For interpretation of the references to colour in this figure legend, the reader is referred to the web version of this article.)

the myocardium does not rule out the involvement of the byproducts of CYP metabolism (i.e., ROS, reactive metabolites), which have been implicated in the mechanism of retene toxicity (Hawkins et al., 2002; Bauder et al., 2005; Hodson et al., 2007b). In addition to CYP1A, the AhR regulates the expression of other CYP enzymes, including CYP1B1, 1C1, and 1C2 (Jönsson et al., 2007), which may contribute to retene metabolism and toxicity.

The evidence for a disruption in erythropoiesis in retene-exposed zebrafish embryos is a particularly interesting finding. More direct assessment of erythrocyte morphology is needed, as the retene-induced erythrocyte shape could also result from cell swelling or may be due to the section angle. However, the general shape of the erythrocytes and reduced erythrocyte numbers are consistent with reports of TCDD-induced disruption of definitive stage erythropoiesis (Belair et al., 2001). Erythropoiesis occurs in two distinct phases in zebrafish, primitive and definitive, which differ both temporally and spatially (see Orkin and Zon, 1997).

4.2. AhR2-dependent and CYP1A-independent toxicity of different PAH compounds

The mechanism of retene toxicity in embryonic zebrafish is AhR2-mediated, but independent of CYP1A activation or activity. These findings are consistent with those reported in TCDD (Prasch et al., 2003; Teraoka et al., 2003; Carney et al., 2004; Dong et al., 2004; Antkiewicz et al., 2006) and benz[*a*]anthracene (Incardona et al., 2006) exposures of zebrafish embryos. Exposures to PCB126 are also mediated by AhR2 (Jönsson et al., 2007). The

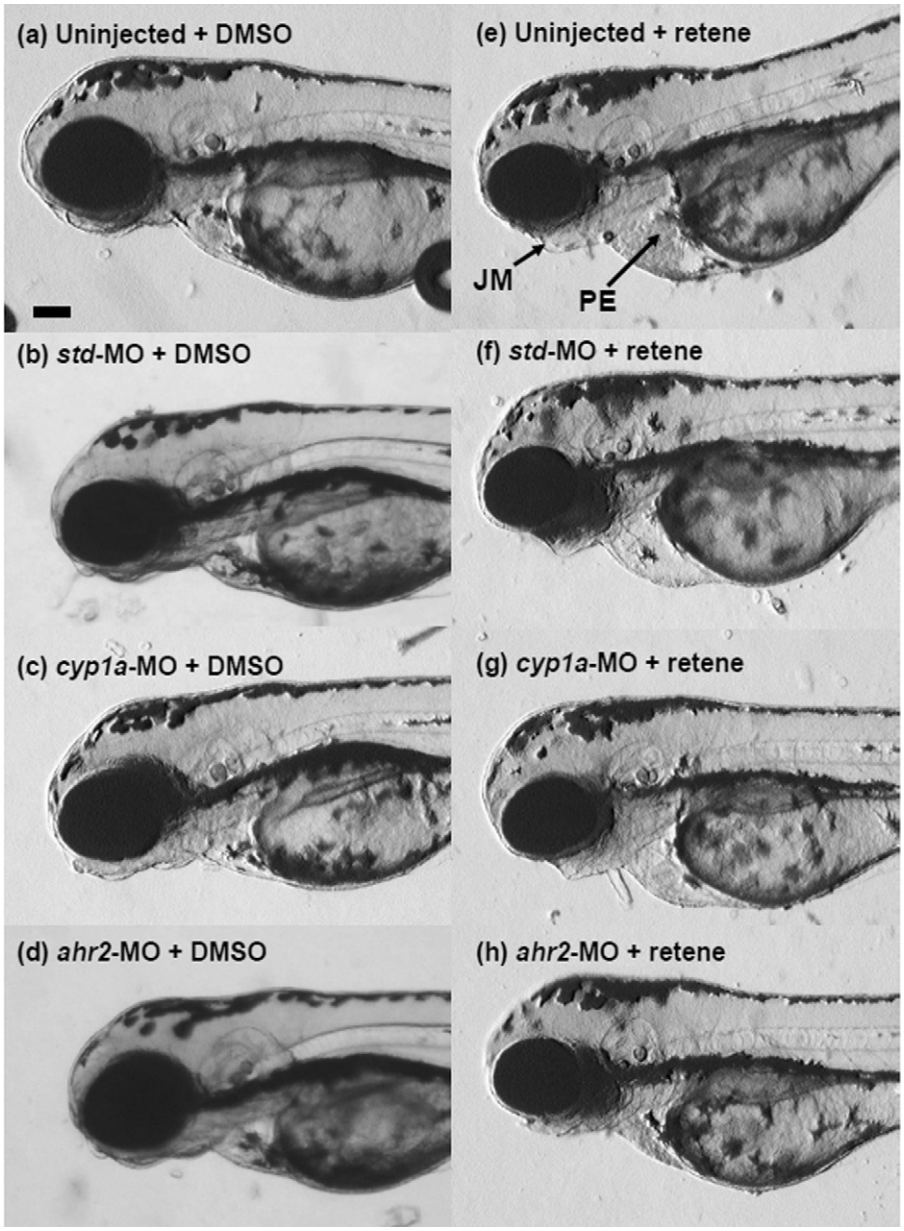

Fig. 6. Effects of retene and DMSO (0.0006%) in uninjected and morpholino-injected zebrafish at 72 hpf. The zebrafish shown are representative of the toxicity observed in >50 embryos for each treatment. PE, pericardial edema; JM, jaw malformation. Scale bar = 0.1 mm.

toxicity of retene also differs from that of other tri- and tetracyclic PAHs (Incardona et al., 2004; Incardona et al., 2005). Notably, phenanthrene (unalkylated retene) exposures produce signs characteristic of atrioventricular conduction block independent of AhR2 (Incardona et al., 2004), illustrating that the addition of alkyl groups can dramatically alter embryotoxicity. These findings have implications for understanding the changing toxicity of crude oil during weathering. The PAH composition of water and tissues are typically dominated by alkyl naphthalenes and parent non-alkylated PAHs such as phenanthrene during early phases of weathering, which shifts to a pattern dominated by higher molecular weight alkyl-PAHs over time (Carls et al., 1999; Heintz et al., 1999; Short and Heintz, 1997). The toxicity of such a mixture in zebrafish embryos is consistent with the AhR-independent effects of the non-alkylated compounds (Incardona et al., 2005). However, as weathering changes the composition to a mixture dominated by C2- and C3-alkylated compounds, the toxicity may shift to include a strong AhR-dependent component, assuming that the alkylated compounds found in crude oils are similar to retene with its isopropyl group.

An AhR-dependent, CYP1A-independent mechanism of retene toxicity is in general agreement with our previous work using chemical inhibition of CYP1A with α-naphthoflavone (ANF; Hodson et al., 2007b; Scott and Hodson, 2008). Co-exposure of rainbow trout embryos to retene and a range of ANF concentrations caused an additive and synergistic toxicity associated with a shift in retene metabolites predominantly from polar to less polar metabolites (Hodson et al., 2007b; Scott and Hodson, 2008). However, the change in toxicity cannot be explained by changes in CYP1A (EROD) activity (Scott and Hodson, 2008). In addition, the toxicity of retene alone is correlated with an increase in CYP1A protein in rainbow trout embryos, suggesting an AhR-mediated toxicity (Scott and Hodson, 2008). Taken together with the results of this study, it appears that the mechanism of retene toxicity is downstream of AhR activation and may be mediated by other AhR-induced CYP isoforms. Studies using a multiple CYP (e.g., *cyp1b1* + *cyp1c1*)

knockdown approach using morpholino oligonucleotides may be an appropriate next step to investigate this further.

Interestingly, CYP1A staining was observed in the vasculature and eye of *ahr2* morphants, which may suggest the presence an additional functional AhR isoform. The resistance of vascular CYP1A induction to *ahr2* knockdown has been observed with other PAHs (Incardona et al., 2005; Incardona et al., 2006). Further studies are needed to investigate this observation as the interpretation is confounded by the potential for cross-reactivity of the CYP1A antibody, and the lack of 100% efficacy of morpholinos.

In conclusion, we find the mechanism of retene toxicity is AhR2-mediated and CYP1A-independent, with the cardiovascular system as the primary target tissue. Further, more direct research is needed to investigate: (i) the specific role of AhR2 in retene-induced cardiovascular toxicity; (ii) the nature of the AhR2-mediated pathological and kinetic differences between retene and organochlorine toxicity; and (iii) the role of other functional AhR and CYP isoforms in xenobiotic toxicity.

Acknowledgements

The authors would like to thank H. Day, S. Fallahtafti, and G.M. Lange for their assistance and ideas, C. Nicol for the use of the microscope and digital camera, T. Linbo for zebrafish husbandry, and K. Peck for critical review of the manuscript. This work was supported by a Natural Sciences and Engineering Research Council Discovery Grant (RGPIN 184288) awarded to PVH, and a Graduate Dean's Travel Grant for Doctoral Research awarded by Queen's University to JAS.

Appendix A. Supplementary data

Supplementary data associated with this article can be found, in the online version, at doi:10.1016/j.aquatox.2010.09.016.

References

Antkiewicz, D.S., Burns, C.G., Carney, S.A., Peterson, R.E., Heideman, W., 2005. Heart malformation is an early response to TCDD in embryonic zebrafish. Toxicol. Sci. 84, 368–377.

Antkiewicz, D.S., Peterson, R.E., Heideman, W., 2006. Blocking expression of AHR2 and ARNT1 in zebrafish larvae protects against cardiac toxicity of 2,3,7,8-tetrachlorodibenzo-*p*-dioxin. Toxicol. Sci. 94, 175–182.

Barry, A., 1948. The functional significance of the cardiac jelly in the tubular heart of the chick embryo. Anat. Rec. 102, 289–298.

Bauder, M.B., Palace, V.P., Hodson, P.V., 2005. Is oxidative stress the mechanism of blue sac disease in retene-exposed trout larvae? Environ. Toxicol. Chem. 24, 694–702.

Belair, C.D., Peterson, R.E., Heideman, W., 2001. Disruption of erythropoiesis by dioxin in the zebrafish. Dev. Dynam. 222, 581–594.

Bendig, G., Grimmler, M., Huttner, I.G., Wessels, G., Dahme, T., Just, S., Trano, N., Katus, H.A., Fishman, M.C., Rottbauer, W., 2006. Integrin-linked kinase, a novel component of the cardiac mechanical stretch sensor, controls contractility in the zebrafish heart. Genes Dev. 20, 2361–2372.

Billiard, S.M., Hahn, M.E., Franks, D.G., Peterson, R.E., Bols, N.C., Hodson, P.V., 2002. Binding of polycyclic aromatic hydrocarbons (PAHs) to teleost aryl hydrocarbon receptors (AHRs). Comp. Biochem. Physiol. B-Biochem. Mol. Biol. 133, 55–68.

Billiard, S.M., Querbach, K., Hodson, P.V., 1999. Toxicity of retene to early life stages of two freshwater fish species. Environ. Toxicol. Chem. 18, 2070–2077.

Brinkworth, L.C., Hodson, P.V., Tabash, S., Lee, P., 2003. CYP1A induction and blue sac disease in early developmental stages of rainbow trout (*Oncorhynchus mykiss*) exposed to retene. J. Toxicol. Environ. Health A 66, 627–646.

Carls, M.G., Meador, J.P., 2009. A perspective on the toxicity of petrogenic PAHs to developing fish embryos related to environmental chemistry. Human Ecol. Risk Assess. 15, 1084–1098.

Carls, M.G., Rice, S.D., Hose, J.E., 1999. Sensitivity of fish embryos to weathered crude oil: Part I. Low-level exposure during incubation causes malformations, genetic damage, and mortality in larval Pacific herring (Clupea pallasi). Environ. Toxicol. Chem. 18, 481–493.

Carney, S.A., Peterson, R.E., Heideman, W., 2004. 2,3,7,8-Tetrachlorodibenzo-*p*-dioxin activation of the aryl hydrocarbon receptor/aryl hydrocarbon receptor nuclear translocator pathway causes developmental toxicity through a CYP1A-independent mechanism in zebrafish. Mol. Pharmacol. 66, 512–521.

Di Giulio, R.T., Benson, W.H., Sanders, B.M., Van Veld, P.A., 1995. Biochemical Mechanisms: metabolism, adaptation and toxicity. In: Rand, G.M. (Ed.), Fundamentals of Aquatic Toxicology: Effects, Environmental Fate, and Risk Assessment, 2nd ed. Taylor Francis, Washington, pp. 523–561.

Dong, W., Teraoka, H., Tsujimoto, Y., Stegeman, J.J., Hiraga, T., 2004. Role of aryl hydrocarbon receptor in mesenphalic circulation failure and apoptosis in zebrafish embryos exposed to 2,3,7,8-tetrachlorodibenzo-*p*-dioxin. Toxicol. Sci. 77, 109–116.

Fernandez-Salguero, P.M., Ward, J.M., Sundberg, J.P., Gonzales, F.J., 1997. Lesions of aryl-hydrocarbon receptor-deficient mice. Vet. Pathol. 34, 605–614.

Forouhar, A.S., Liebling, M., Hickerson, A., Nasiraei-Moghaddam, A., Tsai, H.-J., Hove, J.R., Fraser, S.E., Dickinson, M.E., Gharib, M., 2006. The embryonic vertebrate heart tube is a dynamic suction pump. Science 312, 751–753.

Fragoso, N.M., Hodson, P.V., Kozin, I.S., Brown, R.S., Parrott, J., 1999. Kinetics of mixed function oxygenase induction and retene excretion in retene-exposed rainbow trout (*Oncorhynchus mykiss*). Environ. Toxicol. Chem. 18, 2268–2274.

Grimes, A.C., Erwin, K.N., Stadt, H.A., Hunter, G.L., Gefroh, H.A., Tsai, H.-J., Kirby, M.L., 2008. PCB126 exposure disrupts zebrafish ventricular and branchial but not early neural crest development. Toxicol. Sci. 106, 193–205.

Hahn, M., 1998. The aryl hydrocarbon receptor: a comparative perspective. Comp. Biochem. Phys. C 121, 23–53.

Hawkins, S.A., Billiard, S.M., Tabash, S.P., Brown, R.S., Hodson, P.V., 2002. Altering cytochrome P4501A activity affects polycyclic aromatic hydrocarbon metabolism and toxicity in rainbow trout (*Oncorhynchus mykiss*). Environ. Toxicol. Chem. 21, 1845–1853.

Heintz, R.A., Short, J.W., Rice, S.D., 1999. Sensitivity of fish embryos to weathered crude oil: Part II. Increased mortality of pink salmon (Oncorhynchus gorbuscha) embryos incubating downstream from weathered Exxon Valdez crude oil. Environ. Toxicol. Chem. 18, 494–503.

Henry, T.R., Spitsbergen, J.M., Hornung, M.W., Abnet, C.C., Peterson, R.E., 1997. Early life stage toxicity of 2,3,7,8-tetrachlorodibenzo-p-dioxin in zebrafish (*Danio rerio*). Toxicol. Appl. Pharmacol. 142, 56–68.

Hodson, P.V., Khan, C.W., Saravanabhavan, G., Clarke, L., Brown, R.S., Hollebone, B., Wang, Z., Short, J., Lee, K., King, T., 2007a. Alkyl PAH in crude oil cause chronic toxicity to early life stages of fish. pp. 291–300. In: Proceedings of the 28th Arctic and Marine Oilspill Program Technical Seminar, Environmental Science and Technology Division, Environment Canada, Ottawa, ON, Canada.

Hodson, P.V., Qureshi, K., Noble, C.A.J., Akhtar, P., Brown, R.S., 2007b. Inhibition of CYP1A enzymes by α-naphthoflavone causes both synergism and antagonism of retene toxicity to rainbow trout (*Oncorhynchus mykiss*). Aquat. Toxicol. 81, 275–285.

Hu, N., Sedmera, D., Yost, H.J., Clark, E.B., 2000. Structure and function of the developing zebrafish heart. Anat. Rec. 260, 148–157.

Incardona, J.P., Collier, T.K., Scholz, N.L., 2004. Defects in cardiac function precede morphological abnormalities in fish embryos exposed to polycyclic aromatic hydrocarbons. Toxicol. Appl. Pharmacol. 196, 191–205.

Incardona, J.P., Carls, M.G., Teraoka, H., Sloan, C.A., Collier, T.K., Scholz, N.L., 2005. Aryl hydrocarbon receptor–independent toxicity of weathered crude oil during fish development. Environ. Health Perspect. 113, 1755–1762.

Incardona, J.P., Day, H.L., Collier, T.K., Scholz, N.L., 2006. Developmental toxicity of 4-ring polycyclic aromatic hydrocarbons in zebrafish is differentially dependent on AH receptor isoforms and hepatic cytochrome P450 1A metabolism. Toxicol. Appl. Pharmacol. 217, 308–321.

Incardona, J.P., Carls, M.G., Day, H.L., Sloan, C.A., Bolton, J.L., Collier, T.K., Scholz, N.L., 2009. Cardiac arrhythmia is the primary response of embryonic Pacific herring (*Clupea pallasi*) exposed to crude oil during weathering. Environ. Sci. Technol. 43, 201–207.

Jönsson, M.E., Jenny, M.J., Woodin, B.R., Hahn, M.E., Stegeman, J.J., 2007. Role of AHR2 in the expression of novel cytochrome P450 1 family genes, cell cycle genes, and morphological defects in developing zebra fish exposed to 3,3′,4,4′,5-pentachlorobiphenyl or 2,3,7,8-tetrachlorodibenzo-*p*-dioxin. Toxicol. Sci. 100, 180–193.

Kiparissis, Y., Blazeski, S., Hodson, P., Cai, X., Snieckus, V., 2001. Embryotoxicity of alkyl substituted PAHs. Poster 030. In: Proceedings of the 22nd Annual Meeting of the Society of Environmental Toxicology and Chemistry, Baltimore, Maryland, November 11–15.

Kiparissis, Y., Akhtar, P., Hodson, P.V., Brown, R.S., 2003. Partition Controlled Delivery (PCD) of toxicants: a novel *in vivo* approach for embryotoxicity testing. Environ. Sci. Technol. 37, 2262–2266.

Leppanen, H., Oikari, A., 1999. Occurrence of retene and resin acids in sediments and fish bile from a lake receiving pulp and paper mill effluents. Environ. Toxicol. Chem. 18, 1498–1505.

Linbo, T.L., 2009. Zebrafish (Danio rerio) husbandry and colony maintenance at the Northwest Fisheries Science Center. U.S. Dept. of Commerce, NOAA Tech. Memo., NMFS-NWFSC-100, p. 62.

Männer, J., Thrane, L., Norozi, K., Yelbuz, T.M., 2008. High-resolution in vivo imaging of the cross-sectional deformations of contracting embryonic heart loops using optical coherence tomography. Dev. Dyn. 237, 953–961.

Mehta, V., Peterson, R.E., Heideman, W., 2008. 2,3,7,8-Tetrachlorodibenzo-p-dioxin exposure prevents cardiac valve formation in developing zebrafish. Toxicol. Sci. 104, 303–311.

Orkin, S.H., Zon, L.I., 1997. Genetics of erythropoiesis: induced mutations in mice and zebrafish. Annu. Rev. Genet. 31, 33–60.

Prasch, A.L., Teraoka, H., Carney, S.A., Dong, W., Hiraga, T., Stegeman, J.J., Heideman, W., Peterson, R.E., 2003. Aryl hydrocarbon receptor 2 mediates 2,3,7,8-

tetrachlorodibenzo-*p*-dioxin developmental toxicity in zebrafish. Toxicol. Sci. 76, 128–150.

Scott, J.A., Hodson, P.V., 2008. Evidence for multiple mechanisms of toxicity in larval rainbow trout (*Oncorhynchus mykiss*) co-treated with retene and a-naphthoflavone. Aquat. Toxicol. 88, 200–206.

Short, J.W, Heintz, R.A., 1997. Identification of *Exxon Valdez* oil in sediments and tissues from Prince William Sound and the Northwestern Gulf of Alaska based on a PAH weathering model. Environ. Sci. Technol. 31, 2375–2384.

Teraoka, H., Dong, W., Tsujimoto, Y., Iwasa, H., Endoh, D., Ueno, N., Stegeman, J.J., Peterson, R.E., Hiraga, T., 2003. Induction of cytochrome P450 1A is required for circulation failure and edema by 2,3,7,8-tetrachlorodibenzo-*p*-dioxin in zebrafish. Biochem. Biophys. Res. Comm. 304, 223–228.

Turcotte, T., Akhtar, P., Bowerman, M., Kiparissis, Y., Brown, R.S., Hodson, P.V., 2010. Measuring the toxicity of alkyl-phenanthrenes to early life stages of medaka (*Oryzias latipes)* using partition controlled delivery. Environ. Toxicol. Chem. (accepted with revisions 13/07/2010).

Walisser, J.A., Bunder, M.K., Glover, E., Bradfield, C.A., 2004. Gestational exposure of *Ahr* and *Arnt* hypomorphs to dioxin rescues vascular development. PNAS 101, 16677–16682.